

Final State Interactions Effects in Neutrino-Nucleus Interactions

Tomasz Golan* and Cezary Juszczak
*Institute for Theoretical Physics, Wrocław University
Plac Maxa Borna 9, 50-204 Wrocław, Poland*

Jan T. Sobczyk
Fermi National Accelerator Laboratory, Batavia, Illinois 60510, USA[†]

Final State Interactions effects are discussed in the context of Monte Carlo simulations of neutrino-nucleus interactions. A role of Formation Time is explained and several models describing this effect are compared. Various observables which are sensitive to FSI effects are reviewed including pion-nucleus interaction and hadron yields in backward hemisphere. NuWro Monte Carlo neutrino event generator is described and its ability to understand neutral current π^0 production data in ~ 1 GeV neutrino flux experiments is demonstrated.

I. INTRODUCTION

New generation of neutrino oscillation parameters measurements require a good knowledge of neutrino-nucleus cross sections. Experimental data analysis is always based on predictions from Monte Carlo (MC) event generators [1]. In the 1 GeV energy region, characteristic for several oscillation experiments (MINOS, T2K, Mini-BooNE, NOvA) the use of the Impulse Approximation (IA) picture [2] in which neutrinos scatter on individual quasi-free nucleons is well justified. In this picture any neutrino-nucleus interaction becomes a two-step process: (i) the primary scattering on a bound nucleon, and (ii) Final State Interactions (FSI) affecting the hadrons produced at the step (i). The FSI contribute significantly to the systematic errors in neutrino oscillation measurements so it is important to develop models to describe them better and also to understand the models' limitations [3].

MC codes used in major neutrino oscillation experiments (FLUKA [4], NUANCE [5], NEUT [6], GENIE [7]) in their description of FSI effects rely on the model of intra-nuclear cascade (INC) [8]. It is a semi-classical approach in which some quantum effects can also be incorporated (Pauli blocking, formation time (FT), nucleon correlations). Theoretical arguments for the applicability of the cascade model go back to the works of Glauber [9]. More recently the investigation of the cascade model in the Δ resonance region was done in [10]. The model predictions agree with the experimental data for the pion-nucleus reaction cross sections, including the pion absorption.

While the basic idea behind the models of FSI in the MC codes is always the same, numerical implementations are quite different reflecting priorities of particular neutrino experiments (target, detection technique etc).

An important and not sufficiently understood ingredient in the INC models are Formation Time (FT) effects. On the most fundamental level the FT is related to the Quantum Chromodynamics phenomenon called the color transparency (CT), proposed by Brodsky and Mueller [11]. For high enough four-momentum transfers a quark system is created with a small transverse size (point-like configuration - PLC) which is supposed to suppress hadrons re-interactions. As the typical size of the PLC is of the order of $1/|Q|$ [12], the CT effects are expected to be seen mostly at higher energies. Moreover, two-quark systems are more likely to create PLC than three-quark ones so the effect is expected to be larger for pions, than for nucleons.

Independent phenomenological considerations [13], [14] led to the construction of approximate models of FT. As will be shown in Sect IV many evaluations of basic parameters which determine the size of FT effects have been proposed. It seems important to study them explicitly in the context of neutrino measurements. For example, the FT effects are in the obvious interplay with the pion absorption, reducing its probability in a non trivial momentum dependent way.

A validation of FSI models can be based on any hadronic observables as all of them are FSI sensitive. Such observables include: distributions of numbers of reconstructed hadron tracks, spectra of hadrons in the final state, their angular distributions etc. FSI models used in neutrino MC simulations can also be validated on electro- and photo- nucleus observables. In the analysis of the NOMAD high energy neutrino scattering data [15] the introduction of FT was necessary to get the agreement with the measurements of backward moving protons and pions. It is interesting that the analysis of hadron-nucleus scattering data within INC models indicate that also at lower energies the FT effects can be quite important [16].

In this paper FSI effects are modeled within the NuWro MC event generator [17]. NuWro covers neutrino energy range from a few hundreds MeV (the limit of applicability of the Impulse Approximation - IA) to several TeV. The code has flexibility to include Spectral Function [18] formalism with sophisticated nuclear effects, as an alterna-

* tgolan@ift.uni.wroc.pl

[†] On leave from the Institute for Theoretical Physics, Wrocław University

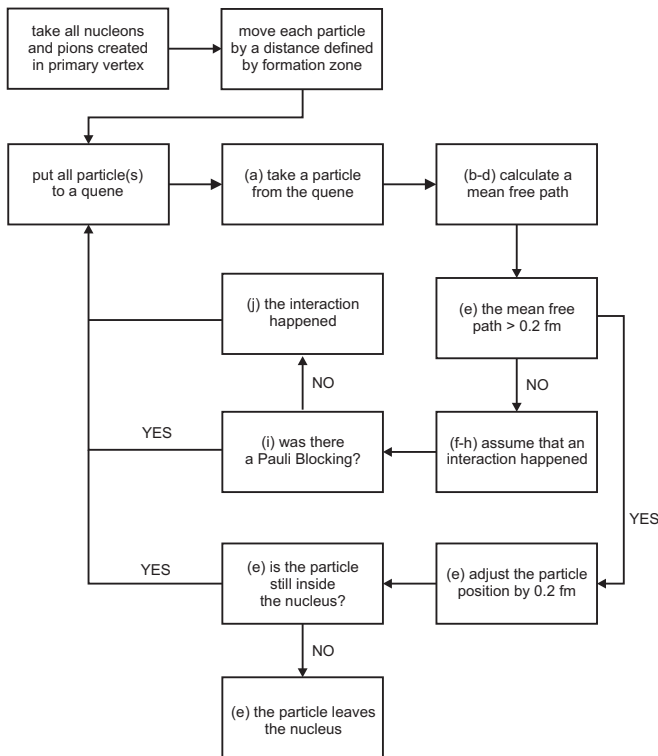


FIG. 1. A block diagram of NuWro INC algorithm.

tive to the Fermi Gas model or an momentum dependent effective potential [19]. NuWro allows for comparisons to the data reported by experimental groups in the FSI effects included format.

We will consider a model of FT which is validated on the NOMAD backward moving pions data. We will then discuss the NC π^0 production data and see how important the FT effects are for the understanding of the experimental data. NC $1\pi^0$ is a very important process because it is a background to $\nu_\mu \rightarrow \nu_e$ oscillation search in water Cherenkov detectors: it can happen that one of two photons from π^0 decay remains undetected and the other is reconstructed as an electron. NC $1\pi^0$ production is also a very useful reaction to validate FSI models in the 1 GeV energy region. It is very sensitive to pion absorption and it is important to investigate how relevant are FT effects making the nuclear environment more transparent for pions produced inside nucleus.

The paper is organized in the following way. In Sect. 2 a general description of the NuWro MC model is given. In Sect. 3 the NuWro FSI model based on the theoretical approach of Oset [10] is described. Several tests are reported showing a good agreement with the original numerical implementation. Sect. 4 contains a summary of various ways to model the FT. Various approaches considered in the context of neutrino interactions and parameters used in theoretical computations and in MC codes are discussed. In Sect 5 the NuWro predictions are compared with the NC $1\pi^0$ production data and the sig-

nificance of the FT effects is discussed. Our conclusions are contained in Sect 6.

II. NUWRO

NuWro is a neutrino event generation software developed at the Wroclaw University [17]. The main motivation for the NuWro authors was to have a tool to investigate the impact of nuclear effects on directly observable quantities with all the FSI effects included. Since 2005 it evolved into a fairly complete neutrino interactions modeling tool. Its basic architecture is similar to better known MCs like NEUT or GENIE. All major neutrino-nucleus interaction channels are implemented and the commonly used relativistic Fermi Gas (FG) model is for certain nuclei replaced with the more realistic Spectral Function model [18]. The NuWro FSI code has recently been updated by implementing the Oset model [10] of effective pion-nucleon cross sections and several options for the FT. Other upgrades include: parameterization of the multipion production cross section in pion-nucleon collisions based on the available data and the implementation of angular distributions in elastic and charge exchange pion-nucleon scattering based on the SAID model [20].

With the inclusion of realistic beam models and a detector geometry module NuWro is becoming a fully-fledged MC event generator ready for use in neutrino experiments.

A. Interactions

In NuWro there are four basic dynamic channels: quasi-elastic (QEL), resonance (RES), more inelastic (DIS) and coherent pion production (COH), each can be either in the charged current (CC) or in the neutral current (NC) mode. The eight channel/mode combinations can be individually enabled or disabled.

For each (but the coherent) channel a particular nucleon which will take part in the interactions is picked up with nuclear matter density used as the probability density. Its momentum is chosen from a ball with the radius set to the Fermi momentum (or the local Fermi momentum calculated for that density in the case of LDA) or obtained as a draw from the Spectral Function.

1. QEL

The CC quasi-elastic and NC elastic reactions are handled by the QEL channel. It uses the standard Llewellyn Smith formulae [21] with several options for the vector form factors (dipole, BBA03 [22], BBBA05 [23], Alberico et al [24]).

The global and local relativistic FG models or SF approach are typically used but the kinematics based on the

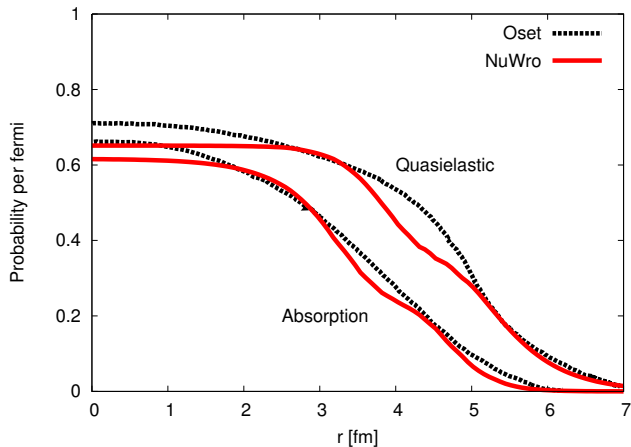


FIG. 2. Probability (per fermi) of microscopic pion-nucleon interactions as a function of a distance from the centre of an iron nucleus. Pion kinetic energy $T_k = 165$ MeV. The Oset model results are taken from [10].

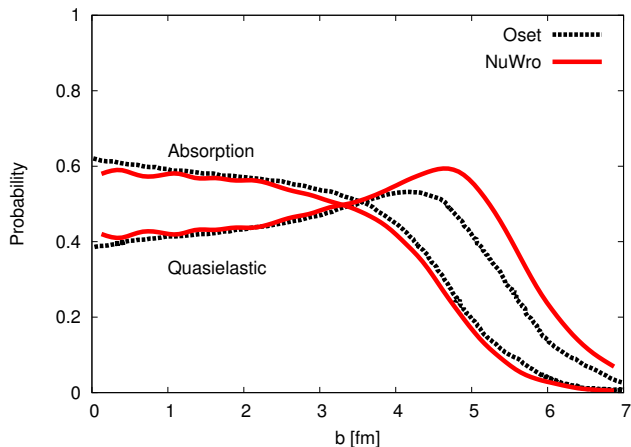


FIG. 3. Probability of macroscopic quasi-elastic or absorption interactions as a function of an impact parameter b for $\pi^{+40}\text{Ca}$ scattering with pion kinetic energy $T_k = 180$ MeV. The Oset model results are taken from [10].

momentum dependent nuclear potential [19] is also available. Currently, the Spectral Functions for carbon, oxygen, argon, calcium and iron are implemented in NuWro according to the tables obtained from Omar Benhar or calculated in [25]. In the SF mode the de Forest kinematical prescription [26] is used.

2. RES

The RES channel is defined as $W < 1.6$ GeV, where W is the invariant hadronic mass. The dominant contribution comes from the single pion production mediated by the $\Delta(1232)$ resonance according to the model [27].

Axial form-factors are taken from the reanalysis of the ANL and BNL bubble chambers data [28]. Not using the standard resonance production Rein-Sehgal model [29] to describe a contribution from higher resonances is justified by the quark-hadron duality hypothesis [30] and by the fact that higher resonances cannot be separated in lepton-nucleus scattering. The non-resonant background is modeled as a fraction of the DIS contribution for $W \in (1.3, 1.6)$ GeV scaled so as the passage to the pure DIS channel be smooth.

3. DIS

The DIS channel is defined as $W > 1.6$ GeV. The total cross sections are evaluated using the Bodek-Yang prescription [31]. The Pythia6 hadronization routine is called for specific quark configurations [32] to allow their meaningful use also in the small W region down to 1.2 GeV.

4. COH

The coherent pion production is implemented using the Rein-Sehgal model [33] with lepton mass corrections.

III. NUWRO FSI MODEL

The NuWro FSI effects are described in a framework of the INC model [8]. The neutrino interaction point is selected inside nucleus according to the nuclear matter density. All secondary hadrons propagate through nucleus and can interact with nucleons inside. In the code the 0.2 fm step length is assumed. For smaller values of the step the results remain the same, only running time increases. Between the collisions hadrons are assumed to be on-shell and move in straight lines. At each point of their path it is decided if there was an interaction or not. This is done based on an effective cross section model. The generic re-interaction algorithm is independent on the dynamics used, also different models of nuclear density can be used. The particular dynamics is taken from the Oset model [10], as it has solid theoretical foundations. The model is supposed to work well in the most important Δ region for pion kinetic energies in the range 85 – 350 MeV. Outside this region the cross sections are obtained from parameterizations of the available pion-nucleon cross section data.

The basic FSI scheme consists in putting nucleons and pions produced in the primary and also in secondary interactions to a queue and repeating the following until the queue gets empty:

- (a) take a particle from the queue,
- (b) examine the nucleus density at its position,

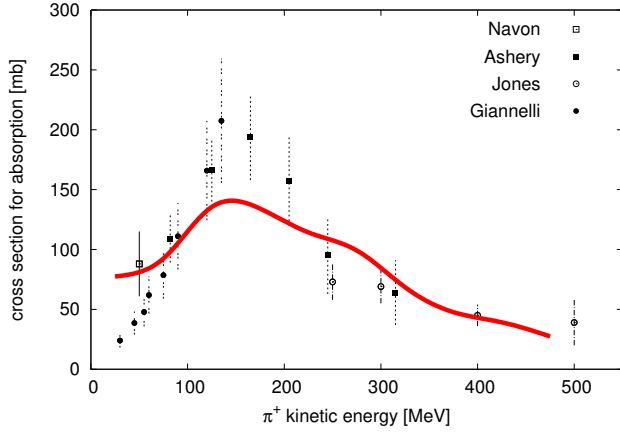


FIG. 4. π^+ ^{12}C absorption cross section. The data points are taken from: Ashery [35], Navon [36], Jones [37] and Giannelli [38]. The solid line shows NuWro predictions.

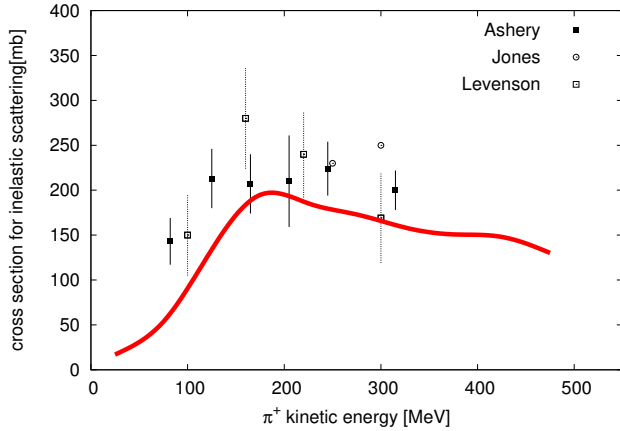


FIG. 5. π^+ ^{12}C inelastic cross section. The data points are taken from: Ashery [35], Jones [37], and Levenson [39]. The solid line shows NuWro predictions.

- (c) calculate the mean free path,
 - (d) probe the exponential distribution for the particle paths,
 - (e) if the selected path is bigger than 0.2 fm adjust the particle position by 0.2 fm,
 - if the particle is still in the nucleus put it at the end of the queue,
 - if the particle is outside the nucleus put it to the list of outgoing particles,
- 1^o nucleons kinetic energy is diminished by the value of the potential:

$$V = \sqrt{M^2 + k_f^2} - M + 8 \text{ MeV}$$

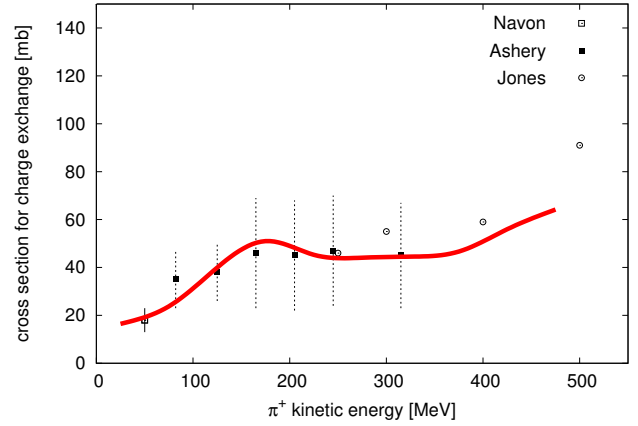


FIG. 6. π^+ ^{12}C charge exchange cross section. The data points are taken from: Ashery [35], Navon [36], and Jones [37]. The solid line shows NuWro predictions.

where k_f is the Fermi momentum and its momentum adjusted so that it remains on the mass shell.

2^o if nucleons kinetic energy is smaller than V the step 1^o cannot be completed. The nucleon is assumed to be unable to leave nucleus. It is reinserted to the nuclear matter and its kinetic energy contributes to the nucleus excitation energy,

- (f) if the selected path is smaller than 0.2 fm assume that interaction with nuclear matter happened at this very place
- (g) probe the target nucleon momentum from the Fermi ball with the local Fermi momentum calculated from the density at that point
- (h) select the type of interaction and generate the kinematics
- (i) check if none of the resulting nucleons is Pauli blocked; in the case of Pauli blocking forget the interaction, reinsert particle to the queue at the failed interaction point (Pauli blocking effects can be also included by means of increased values of the mean free paths and then this step of the algorithm must be skipped)
- (j) if the interaction was not Pauli blocked, all the particles in the final state are put to the end of the queue.
- (k) if FT/FZ effects apply also to secondary interactions (this is model dependent) the particles positions are accordingly adjusted.

The nucleus radius is defined as a distance from the center, where the density is smaller by a factor of 10^4 than the maximal one.

As a result of some nucleons joining the INC, the nuclear matter density is reduced but the shape of the density profile is assumed to be unchanged.

A. The Oset model

On the microscopic level the Oset model includes the quasi-elastic pion-nucleon reaction (including the charge exchange channel) and the pion absorption with two- and three-body absorption mechanisms. The interaction probability per time unit is:

$$P dt = -\frac{1}{\omega} \text{Im}(\Pi) dt = -2 \text{Im}(V_{opt}) dt \quad (1)$$

where ω is the pion energy, Π is the pion self-energy, and V_{opt} is the optical potential.

In the simplest case of $\pi^+ p \rightarrow \pi^+ p$ p-wave scattering calculations lead to the result:

$$P = \frac{1}{\omega} \frac{2}{3} \left(\frac{f^*}{m_\pi} \right)^2 q_{c.m.}^2 |G_\Delta(q)|^2 \frac{1}{2} \Gamma \rho_p \quad (2)$$

where f^* is $\pi N \Delta$ coupling constant ($f^{*2}/4\pi = 0.36$), m_π is the pion mass, $q_{c.m.}$ is the pion momentum in the centre of mass system, G_Δ is Δ propagator, Γ its width and ρ_p is proton density.

An important in-medium effect is the Δ self-energy. Its imaginary part can be parameterized as [34]:

$$\text{Im} \Sigma_\Delta(\omega) = - [C_Q(\rho/\rho_0)^\alpha + C_{A2}(\rho/\rho_0)^\beta + C_{A3}(\rho/\rho_0)^\gamma] \quad (3)$$

The Δ width is modified $\frac{1}{2}\tilde{\Gamma} \rightarrow \frac{1}{2}\tilde{\Gamma} - \text{Im} \Sigma_\Delta$, changing the Δ propagator and producing extra terms in Eq. (2), proportional to functions C 's present in Eq.(3). The term proportional to C_Q corresponds to higher order quasi-elastic scattering and the terms with C_{A2} and C_{A3} correspond to two- and three-body absorption. ρ is the nuclear matter density and $\rho_0 = 0.17 fm^{-3}$ is the normal density.

The final expression for the interaction probability in the nuclear matter is:

$$P = \frac{1}{\omega} \int \frac{d^3k}{(2\pi)^3} n(\vec{k}) \frac{2}{3} \left(\frac{f^*}{m_\pi} \right)^2 q_{c.m.}^2 |G_\Delta(q+k)|^2 \frac{1}{2} \tilde{\Gamma}(q+k) \quad (4)$$

where $n(\vec{k})$ is the occupation number for protons/neutrons.

The Δ self-energy depends strongly on the nuclear density and the pion absorption is more likely to occur in the central part of the nucleus.

Finally, one introduces improvements to the model coming from: the πN interaction s-wave contribution, the real part of the optical potential and finite size effects.

	$T_\pi = 85 \text{ MeV}$			$T_\pi = 245 \text{ MeV}$			
	n=1	n=2	n=3	n=1	n=2	n=3	n=4
Oset	0.90	0.09	0.01	0.69	0.25	0.05	0.01
NuWro	0.89	0.10	0.01	0.67	0.24	0.07	0.02

TABLE I. Probabilities that macroscopic quasi-elastic process proceeds through n microscopic collisions. Oset model results are taken from [10].

	$T_\pi = 85 \text{ MeV}$			$T_\pi = 245 \text{ MeV}$			
	n=0	n=1	n=2	n=0	n=1	n=2	n=3
Oset	0.81	0.17	0.02	0.37	0.41	0.17	0.04
NuWro	0.87	0.12	0.01	0.41	0.37	0.16	0.05

TABLE II. Probabilities that pion absorption occurs after n th quasi-elastic microscopic scatterings. Oset model results are taken from [10].

B. NuWro implementation of the Oset model

The Oset model is implemented in NuWro by means of tables containing the cross-sections as the functions of pion kinetic energy at various nuclear matter densities. Because finite size effects are not universal it was necessary to prepare tables for each isotope separately.

In the analysis of the performance of the cascade model one should distinguish microscopic (pion-nucleon) and macroscopic (pion-nucleus) reactions. Figs 2-3 show a comparison between our implementation and the original Oset model. Fig. 2 shows the inverse of mean free paths (or equivalently: interaction probabilities per fermi) for two microscopic interactions as functions of the distance from a nucleus center. In both cases contributions from pion-proton and pion-neutron reactions are added. There is a significant dependence on the nuclear density: in the nucleus central region the absorption probability is large. In the peripheral region the quasi-elastic scattering dominates overwhelmingly. Fig. 3 shows probabilities of macroscopic processes as functions of the impact parameter. One can see that for small values of the impact parameter the absorption is more likely than the quasi-elastic scattering. One should remember that an incident pion can be absorbed also after one or more microscopic quasi-elastic scatterings.

Tables I-II help to understand other aspects of $\pi^+ {}^{12}\text{C}$ scattering. Again, we compare results from the original Oset paper with the NuWro implementation. Table I presents the probabilities that a macroscopic quasi-elastic event proceeds through n collisions. Table II contains the probabilities that absorption occurs exactly after n microscopic quasi-elastic pion scatterings. The results are shown for two values of incident pion kinetic energy: 85 and 245 MeV. More energetic pions are likely to undergo several scatterings in which they lose a fraction of their energy until they fall into the absorption peak in the Δ

region.

With a satisfactory agreement for microscopic ingredients of the Oset model, we present a comparison of the NuWro cascade model predictions with experimental data for the $\pi^+ {}^{12}\text{C}$ scattering (Figs 4 – 6).

One can distinguish the following macroscopic pion-nucleus reactions: elastic, charge exchange, absorption, and inelastic scattering. We do not show the results for the double charge exchange reaction because the cross section is very small. For larger energies the inelastic cross section contains a pion production component.

The cross section measurement of the charge exchange and absorption processes is straightforward. The inelastic cross section is obtained in the indirect way as:

$$\sigma_{inel} = \sigma_{total} - \sigma_{elastic} - (\sigma_{absorption} + \sigma_{CEX}), \quad (5)$$

where the elastic pion-nucleus cross section contribution is evaluated based on theoretical and experimental arguments (for the details see [35]).

The NuWro predictions are obtained in the standard way by arranging a homogeneous flux of pions and counting the particles in the final state assuming that at least one microscopic interaction took place. In the simulations on carbon the impact parameter is limited to $b < 6.5$ fm. We checked that with larger b values the evaluated cross sections do not change. In the MC simulations one cannot model elastic pion-nucleus reaction. The sum over all possible interaction channels gives the pion-nucleus reaction cross section.

Figs 4-6 show that the NuWro predictions are in a good agreement with the data.

FT effects can be also used in the secondary interaction but their impact on the final results is very small.

IV. FORMATION TIME/ZONE

A. Generalities

The concept of the Formation Time/Formation Zone (FT/FZ) was introduced by Landau and Pomeranchuk [40] in the context of multiple scattering of electrons passing through a layer of material. In the LAB frame the FT is given as:

$$t = \frac{E}{k \cdot p} \quad (6)$$

where $p^\mu = (E, \vec{p})$ and $k^\mu = (\omega, \vec{k})$ are four-momenta of the electron and the emitted photon respectively. t has the interpretation of the minimal time necessary for a photon to be created.

The idea of FT was applied to hadron production by Stodolsky [13], who considered the multiproduction of mesons by protons passing through a nucleus. In the Eq. 6 he replaced the electron by a projectile hadron

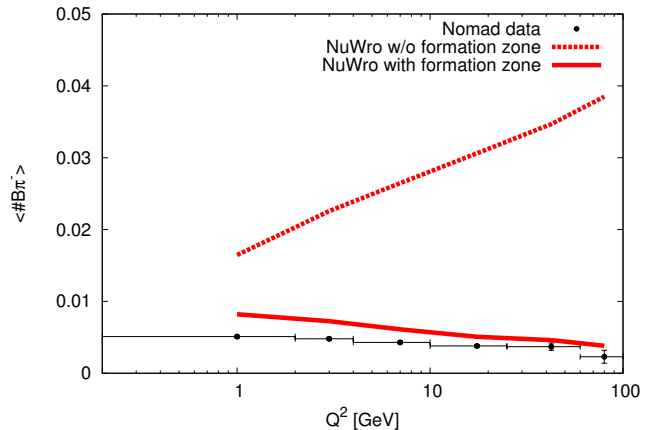


FIG. 7. Average number of backwards going pions as a function of Q^2 in the NOMAD experiment.

with a four-momentum $p_0^\mu = (E_0, 0, 0, \sqrt{E_0^2 - M_0^2})$ and the photon by a secondary hadron with a four-momentum $p^\mu = (E, \vec{p}_T, \sqrt{E^2 - p_T^2 - M^2})$ obtaining:

$$\begin{aligned} t \rightarrow t_f &= \frac{E_0}{EE_0 - \sqrt{E^2 - p_T^2 - M^2}\sqrt{E_0^2 - M_0^2}} \\ &= \frac{1}{E \left(1 - \sqrt{1 - \frac{\mu_T^2}{E^2}} \sqrt{1 - \frac{M_0^2}{E_0^2}} \right)} \end{aligned} \quad (7)$$

where μ_T is the transverse mass defined as $\mu_T^2 \equiv M^2 + p_T^2$.

For higher energies $E \gg \mu_T$, $E_0 \gg M_0$ and

$$t_f \approx \frac{2E}{(M_0 x)^2 + \mu_T^2} \quad (8)$$

where $x = \frac{E_0}{E}$. Rantf [14] argued that a further simplification $x \approx 0$ is usually well justified and finally in the LAB frame:

$$t_f \approx \frac{2E}{M^2 + p_T^2} \quad (9)$$

and in the hadron's rest frame:

$$t_{f,rest} \approx \frac{2M}{M^2 + p_T^2}. \quad (10)$$

Inspired by this expression Rantf postulated another formula for the FT in the hadron rest frame. He kept the basic relativistic character of the FT but introduced an arbitrary parameter τ_0 to control its size:

$$\tau_{rest} = \tau_0 \frac{M^2}{M^2 + p_T^2}. \quad (11)$$

The FT defined in Eq. 11 was implemented in the MC event generator DPMJET [41] which later became a part of the FLUKA code and was used by the NOMAD collaboration [42]. In the DPMJET cascade model the FT is applied to hadrons resulting from all the interaction modes: QEL, RES and DIS. Following the ideas of Bialas [43] in DPMJET values of FT are sampled from the exponential distribution.

The FT played an important role in the NOMAD analysis of the CCQE events [15]. They populate mainly one- and two- tracks samples. A change of τ_0 modifies the MC predictions for the size of both samples: an increase of FT makes an impact of the FSI effects on the ejected protons smaller and they are more likely to have larger momentum with increased probability of being detected and populating the two-track sample of events. By adjusting the size of the formation time the values of M_A calculated independently from either of the two samples of events became almost identical.

In the above estimations of the FT effect several assumptions were made which are not necessarily valid at lower energies. This is taken into account in the more recent low energy FLUKA cascade model, called PEANUT [44]. In the case of the QEL reaction the concept of coherence length (CL) was proposed to substitute the FT effect.

Derivation of the CL is based on the uncertainty principle arguments: Let p^μ be the outgoing nucleon four-momentum and $q^\mu = (\omega, \vec{q})$ the four-momentum transfer, both in the LAB frame. Because $p \cdot q$ is a Lorentz scalar, one can calculate $\tilde{\omega}$ ($\tilde{\omega}$ denotes quantities calculated in the nucleon rest frame), the energy transfer in the final nucleon rest frame:

$$|p \cdot q| = |\vec{p} \cdot \vec{q}| = |\tilde{\omega} M| \Rightarrow |\tilde{\omega}| = \frac{|p \cdot q|}{M} \quad (12)$$

From the uncertainty principle $\tilde{\omega}$ can be used to estimate the reaction time in the nucleon's rest frame and then in the LAB frame as well. Within that time the nucleon is assumed to be unable to re-interact [45]:

$$t_{CL,rest} = \frac{M}{|p \cdot q|} \quad t_{CL} = \frac{E}{|p \cdot q|}, \quad (13)$$

Surprisingly, the Landau-Pomeranchuk formula Eq. 6 is reproduced.

Among other approaches to give a quantitative evaluation of the FT effects one should mention the SKAT parameterization of the LAB frame FZ [46]:

$$l_{SKAT} = \frac{|\vec{p}|}{\mu^2}. \quad (14)$$

The value of the free parameter was found to be $\mu^2 = 0.08 \pm 0.04 \text{ GeV}^2$ based on the experimental data for the multiplicity of low momentum ($300 \text{ MeV}/c < p <$

$600 \text{ MeV}/c$) protons. This value of μ^2 agrees also with the analysis of the momentum distribution of negatively charged mesons in the region $p < 3 \text{ GeV}/c$.

The SKAT formula can be translated to the following value of FT:

$$t_{SKAT} = \frac{E}{|\vec{p}|} l_{SKAT} = \frac{E}{\mu^2}, \quad t_{SKAT,rest} = \frac{M}{\mu^2}. \quad (15)$$

Compared to the Rantf formula (Eq. 11) the SKAT parameterization corresponds to $p_T = 0$ but it also introduces a scale proportional to the hadron mass: $\tau_0 \leftrightarrow M/\mu^2$. According to the SKAT parameterization FZ is identical for pions and nucleons with the same momentum. At $p \sim 1 \text{ GeV}/c$ FZ is expected to be $\sim 2.5 \text{ fm}$, which is of the size of the carbon nucleus.

In another approach to model FT effects, at a distance z from the interaction point one postulates an effective (reduced) hadron-nucleon interaction cross section [47]:

$$\sigma_{eff}(z) = \sigma_{free} \left(1 - e^{-z M m_0 / |\vec{p}|}\right) \quad (16)$$

with $m_0 \approx 0.4 \text{ GeV}$.

Similar description of the FT effects (reduction of the cross section) is used in the quantum diffusion model [48]:

$$\sigma_{hN}^{eff}(z) = \sigma_{hN} \times \left[\left(\frac{z}{l_h} + \frac{\langle n^2 k_t^2 \rangle}{Q^2} \left(1 - \frac{z}{l_h}\right) \right) \theta(l_h - z) + \theta(z - l_h) \right], \quad (17)$$

where σ_{hN} is the free hadron-nucleon cross section, z is the distance from the interaction point, $k_t^2 \cong 0.35 \text{ MeV}/c$ is the average quark transverse momentum, $n = 2, 3$ for pions and nucleons. The size of FT is determined by l_h which can be evaluated to be

$$l_h = 2p_h \left\langle \frac{1}{M_n^2 - M_h^2} \right\rangle, \quad (18)$$

where p_h and M_h denote hadron momentum and mass, and M_n is an intermediate state mass. The precise value of $\Delta M^2 = M_n^2 - M_h^2$ is not known and is estimated to be between 0.25 and 1.4 GeV^2 . In [49] the values of 1 GeV^2 and 0.7 GeV^2 are used for protons and pions.

In the parameterizations given in Eqs (16) and (17) smaller effective cross section translates into a larger average distance to the first reinteraction point.

In the case of pions produced via the Δ excitation and decay there is still another natural way to model the FT effect. In the INC picture we can treat the Δ (like in the GiBUU approach [50]) as a real particle propagating some distance before it decays. The Δ lifetime in its rest frame is equal $\frac{1}{\Gamma}$, with $\Gamma \approx 120 \text{ MeV}$, so in the LAB frame one obtains:

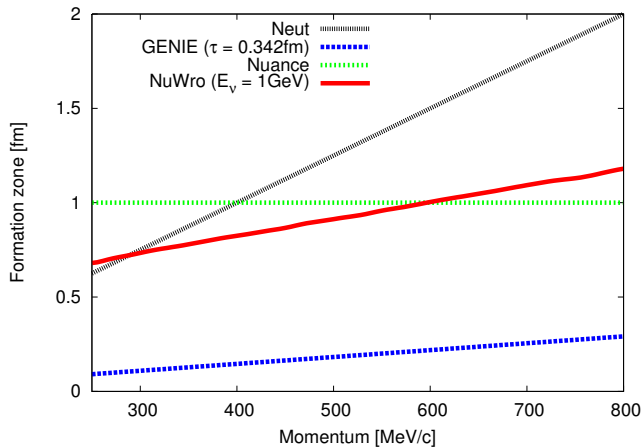


FIG. 8. Nucleon Formation Zone in the LAB frame as a function of its momentum.

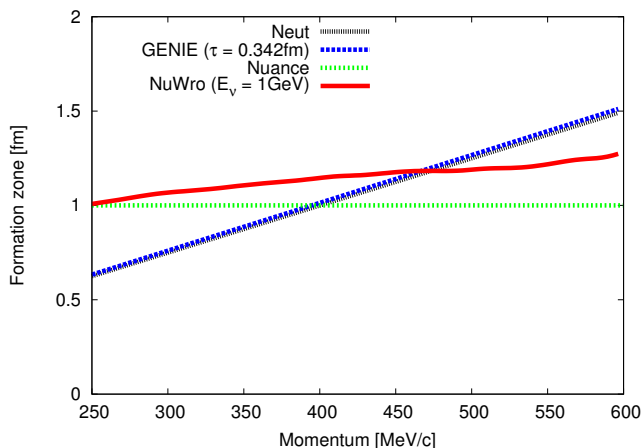


FIG. 9. Pion Formation Zone in the LAB frame as a function of its momentum

$$t_{\Delta} = \frac{E_{\Delta}}{MT} \quad (19)$$

where E_{Δ} is the Δ energy in the LAB frame.

We conclude that various approaches lead to similar expressions for the FT as far as the dependence on hadron momentum is concerned but numerical coefficient and the size of the effect can be quite different.

B. FT models in MC event generators

Table III summarizes available information about FT models in major neutrino MC event generators.

NEUT uses the SKAT model both for RES and DIS [51].

MC	QE	RES ^a	DIS
NEUT	–	SKAT	SKAT
FLUKA	Coh length	Rantf	Rantf
GENIE	–	–	Rantf-like
NUANCE	1 fm	1 fm	1 fm

^a Note that every MC has its own slightly different definition of what does RES and DIS terms mean.

TABLE III. FT models in MC event generators

FLUKA uses Eq. 13 for quasielastic scattering and Eq. 11 for other processes.

GENIE uses Eq. 11 but in a simplified form, neglecting p_T :

$$t_{\text{Genie}} = \tau_0. \quad (20)$$

GENIE assumes the value $\tau_0 = 0.342 \text{ fm}/c$ [52]. One can check that for the pions the SKAT formula is reproduced. GENIE applies FZ to DIS events and also to the non-resonant background events in the RES dynamics [53].

NUANCE implemented an effective model in which the FZ is always equal to 1 fm [54].

C. NuWro FT model

In NuWro the formation zone effects are implemented:

- as coherence length (Eq. 13) for quasielastic scatterings
- as Δ propagation (Eq. 19) for RES interactions
- using Rantf model (Eq. 11) with some parameter τ for DIS

There is a smooth transition between the last two models at $W \simeq 1.6 \text{ GeV}$.

With the Rantf model (without the approximation $p_T = 0$) the average value of the FT depends both on neutrino energy and on hadron momentum. For a fixed value of the neutrino energy, lower hadron momenta typically correspond to larger values of the transverse momentum and smaller values of the FT.

In order to fix the value of the parameter τ we analyze the NOMAD data for the backward moving pions.

1. Comparison with NOMAD measurement of backward moving pions

To fine tune our model of FZ we make use of the NOMAD experimental data [55]. The average neutrino energy in NOMAD is $\langle E_{\nu} \rangle = 24 \text{ GeV}$ and the target composition is dominated by carbon (64.30%) and oxygen (22.13%) with small additions of other elements.

Scenario	Without formation zone	With formation zone
1	37.2%	83.7%
2	43.3%	15.5%
2a	22.0%	8.1%
2b	15.6%	7.4%
2c	5.8%	0%
3	2.7%	0.7%
3a	1.9%	0.6%
3b	0.8%	0.1%
4	16.7%	0.1%

TABLE IV. Contribution to events with backward π^- from different scenarios (description in text)

We focus on the pion data. Our main observable is the average number of backward moving ($\cos\theta_{LAB} < 0$) negative pions $B\pi^-$ with the momentum p_π between 350 and 800 MeV/c, as a function of Q^2 . This observable is very sensitive to the FSI effects. Without FSI the number of backward moving pions would be very small because they appear mainly due to nuclear reinteractions. Introduction of the FT makes the FSI effects smaller and reduces the number of $B\pi^-$.

Simulations made for various values of τ lead us to the conclusion that a good agreement with the data is obtained with $\tau \sim 8$ fm/c. Fig. 7 shows average numbers of backward moving π^- reported by NOMAD, and predicted by NuWro with and without FZ, as a function of Q^2 . In order to better understand the NuWro performance we analysed various ways in which $B\pi^-$ appear:

1. pions are created in the primary vertex and undergo quasielastic scatterings during FSI
2. pions are created during FSI in pion-nucleon interactions
 - (a) single pion production
 - (b) double pion production
 - (c) triple pion production
3. pions are created during FSI in nucleon-nucleon interactions
4. there are more pion production processes during FSI.

Contributions from the above scenarios to events with backward moving π^- are listed in Table IV.

Table V shows distributions of the number of $B\pi^-$ in a single event. The NuWro predictions (with and without the FZ) are compared with the Nomad data [55].

2. Comparison with other MC event generators

Figs 8 and 9 show the values of the FZ in NuWro compared to other MC neutrino event generators. It is interesting that in the case of pions various models of the

$\langle \#B\pi^- \rangle$	Data	NuWro	
		Without FT	With FT
0	939617	921048	937883
1	4238	22590	6126
2	164	375	8

TABLE V. Contribution to $B\pi^-$ coming from events with 0, 1 or 2 pions

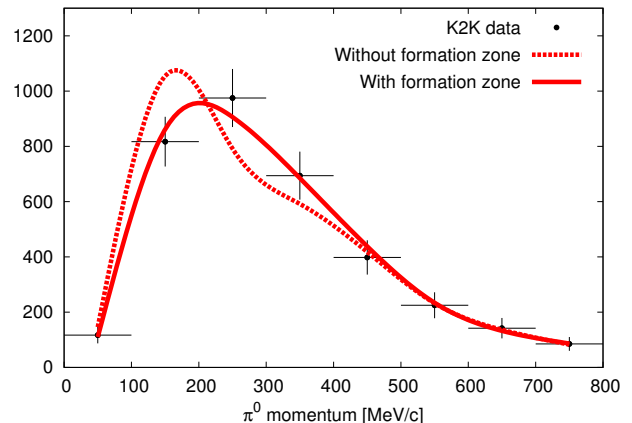


FIG. 10. K2K: NC $1\pi^0$ production as a function of π^0 momentum; the data and NuWro predictions are normalized to the same area.

FZ give very similar results, while in the case of nucleons the differences are much larger.

The NuWro results are given for a specific neutrino energy ($E_\nu = 1\text{GeV}$). The FZ grows with E_ν due to the transverse momentum in the denominator, which goes to zero when hadron energy becomes higher.

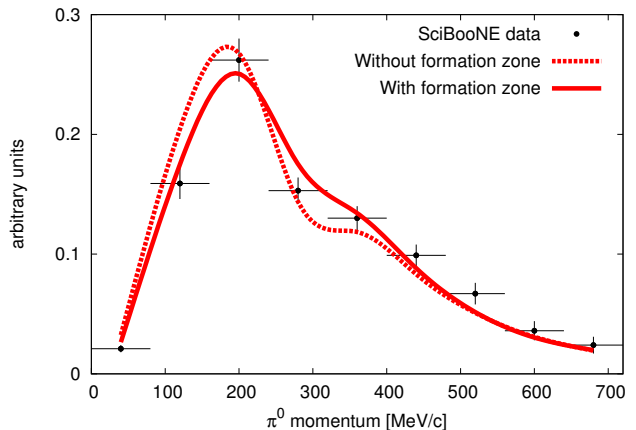


FIG. 11. SciBooNE: NC π^0 production as a function π^0 momentum; the data and NuWro predictions are normalized to the same area.

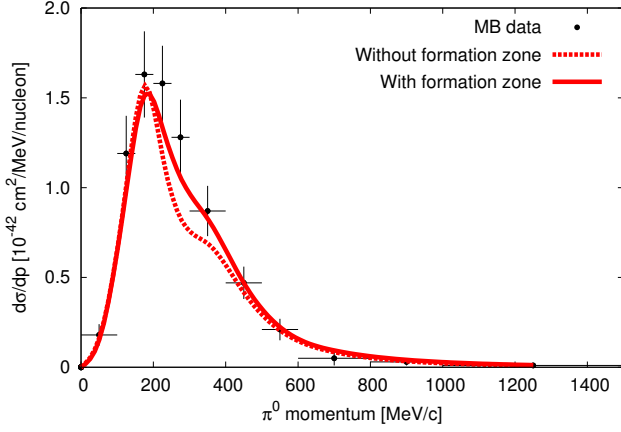


FIG. 12. MiniBooNE (neutrino mode): NC $1\pi^0$ production as a function π^0 momentum.

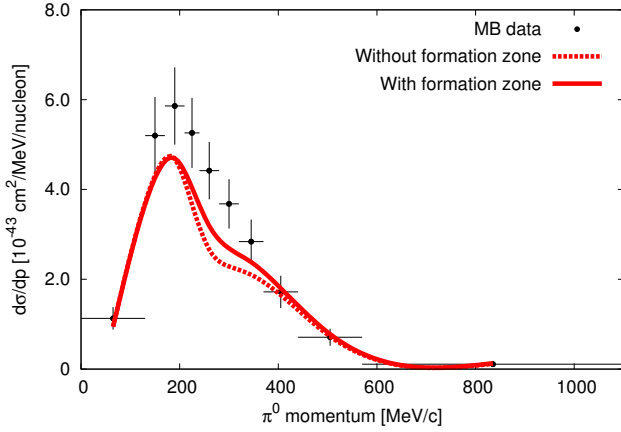


FIG. 13. MiniBooNE (anti-neutrino mode): NC $1\pi^0$ production as a function π^0 momentum.

In NuWro the dependence of the FZ on the pion kinetic energy is very flat.

V. APPLICATION: NC $1\pi^0$ PRODUCTION

A. Free nucleon NC π^0 production

The data for NC $1\pi^0$ production cross section on a free nucleon target is very scarce. The only such measurement so far was done in the Gargamelle bubble chamber. The target was in fact composed of C_3H_8 (90%) and CF_3Br but the FSI effects were subtracted according to the model in [58].

In view of large uncertainties in the understanding of nuclear effects the results should be treated with some caution. We notice also that the data contain a contribution from the COH reaction. Originally, the results

Channel	Cross section per nucleon ($\times 10^{-38} \text{ cm}^2$)		
	Data	NuWro	
		free nucleon	bound nucleon
$\nu_\mu p \rightarrow \nu_\mu p \pi^0$	0.13 ± 0.02	0.15	0.12
$\nu_\mu n \rightarrow \nu_\mu n \pi^0$	0.08 ± 0.02	0.17	0.14
$\nu_\mu p \rightarrow \nu_\mu n \pi^+$	0.08 ± 0.02	0.13	0.11
$\nu_\mu n \rightarrow \nu_\mu p \pi^-$	0.11 ± 0.03	0.14	0.13
$\nu_\mu n \rightarrow \mu p \pi^0$	0.24 ± 0.04	0.38	0.36

TABLE VI. Single pion production cross sections

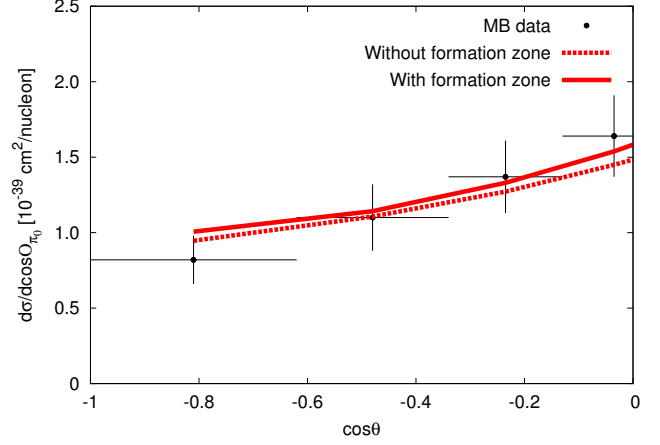


FIG. 14. MiniBooNE (neutrino mode): NC $1\pi^0$ production as a function $\cos\theta$.

were presented as efficiency corrected relative production rates in several pion production channels [56]. The data re-analysis was done in [57]: information about neutrino flux was taken into account and the cross sections estimations were done.

Table VI shows the experimental data from [57] and NuWro predictions obtained for neutrinos of energy 2.2 GeV on free nucleon target and also on nucleons bound in ^{12}C , with Pauli blocking and Fermi motion effects taken into account but without FSI effects. We find the agreement to be satisfactory. It is also possible to compare the NuWro predictions and the data for relative contributions from RES and DIS reaction channels. In the case of $\nu p \rightarrow \nu p \pi^0$ reaction the NuWro predictions for the RES:DIS ratio are: 78 : 22 for free and 82 : 18 for bound nucleons. The experimental data are $\sim 80 : 20$ (see Fig. 11 in [56]).

B. NC $1\pi^0$ production on a nucleus

The recent experimental data for NC π^0 production come from three experiments. Basic information about them is summarized in Table VII.

In the K2K and MiniBooNE (MB) experiments the signal was defined as exactly one π^0 leaving the nucleus

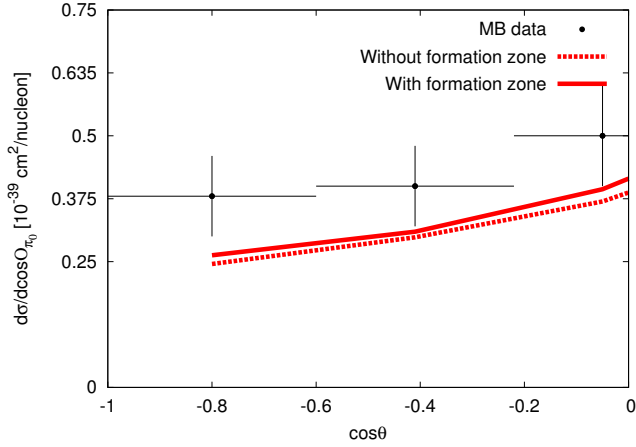


FIG. 15. MiniBooNE (anti-neutrino mode): NC $1\pi^0$ production as a function $\cos\theta$.

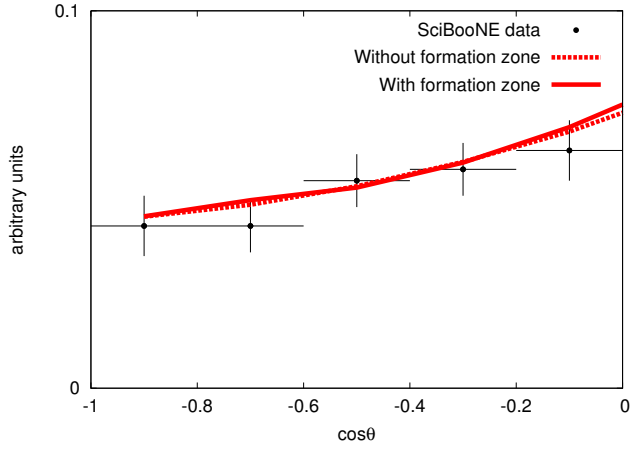


FIG. 16. SciBooNE: NC π^0 production as a function $\cos\theta$.

target and no other mesons in the final state. In the case of SciBooNE (SciB) the signal was defined as *at least one* π^0 in the final state, with possible other pions as well.

The experimental signal for $1\pi^0$ production comes from: (i) single π^0 produced at the interaction point in the single pion production reaction; (ii) π^0 produced in double pion production reaction with other pion being absorbed; (iii) single π^\pm production with charge exchange reaction $\pi^\pm \rightarrow \pi^0$ inside nucleus; (iv) primary quasi-elastic reaction with π^0 being produced due to nucleons re-interactions inside nucleus. For the $2\pi^0$ production the number of possible scenarios is even bigger.

According to NuWro, most of the $1\pi^0$ signal events (93 – 95%) come from the initial RES single pion production reactions, see Table VIII. In the case of the MB antineutrino flux the contribution is the smallest, because the antineutrinos are on average less energetic. Also the impact of the FZ is in clear anti-correlation with the average flux energy.

Experiment	Beam	$\langle E_\nu \rangle$ [GeV]	Target	Normaliz.	Measurement
K2K [59]	ν_μ	1.30	H_2O	relative	dN/dT_π
MB [60]	ν_μ	0.81	CH_2	absolute	$d\sigma/dT_\pi$, $d\sigma/d\cos\theta_\pi$
MB [60]	$\bar{\nu}_\mu$	0.66	CH_2	absolute	$d\sigma/dT_\pi$ $d\sigma/d\cos\theta_\pi$
SciB [61]	ν_μ	0.81	C_8H_8	relative	dN/dT_π $dN/d\cos\theta_\pi$

TABLE VII. Recent NC π^0 production measurements.

Channel	K2K	MB ν	MB $\bar{\nu}$
$1\pi^0 \rightarrow 1\pi^0$	93.1% (84.5%)	93.0% (88.3%)	94.8% (92.4%)
$\text{no } \pi \rightarrow 1\pi^0$	2.0% (3.2%)	1.8% (2.4%)	1.2% (1.6%)
other $\pi \rightarrow 1\pi^0$	3.7% (6.8%)	4.2% (5.8%)	3.2% (3.9%)
more $\pi \rightarrow 1\pi^0$	1.2% (5.5%)	1.0% (3.5%)	0.7% (2.1%)

TABLE VIII. Origin of the events with $1\pi^0$ in the final state. Values in brackets refer to results without FT.

Table IX enumerates what can happen to a π^0 produced in the primary vertex due to the FSI effects. One can see that pion absorption (the second row) reduces the number of NC π^0 events, but the FZ makes the effect much smaller. Also the charge exchange reaction (the third row) has a significant impact on the final states. It is clear that the NC π^0 production measurement is a very good test for the FSI models in MC event generators.

Table X shows the composition of the π^0 signal in the SciB experiment as it is understood by NuWro. The second column contains the values reported by the SciB collaboration obtained from the MC they used in the data analysis (NEUT).

K2K and SciBooNE did not publish the normalized differential cross section. However, flux averaged ratios of NC π^0 to total CC cross sections were given. In the Table XI we compare both values with the NuWro results.

Figures 10 - 13 show the data and NuWro predictions for π^0 momentum distribution in various experiments.

In the case of the normalized cross section the main effect of the introduction of the FZ is the increase of the cross section in the pion absorption peak region. The effect can be estimated to be 10 – 15%. In the case of the K2K measurement the use of the FZ also moves the

Channel	K2K	MB ν	MB $\bar{\nu}$
$1\pi^0 \rightarrow 1\pi^0$	81.6% (64.0%)	79.1% (66.9%)	83.0% (74.5%)
$1\pi^0 \rightarrow \text{no } \pi$	5.9% (19.3%)	7.2% (19.2%)	6.4% (15.9%)
$1\pi^0 \rightarrow \text{other } \pi$	10.1% (11.0%)	10.2% (10.1%)	9.6% (7.8%)
$1\pi^0 \rightarrow \text{more } \pi$	2.4% (5.7%)	2.0% (3.7%)	1.0% (1.8%)

TABLE IX. Impact of FSI effects on the events with $1\pi^0$ in the primary interaction. Values in brackets refer to the results without FT.

Channel	SciB MC	NuWro (no FT)	NuWro (FT)
$1\pi^0$	85%	80%	82%
$1\pi^0 + \text{charged } \pi$	11%	16%	14%
$2\pi^0$	4%	4%	4%

TABLE X. Predictions of contribution to π^0 channel from SciBooNE MC and NuWro

NC π^0 /CC	K2K	SB
Data	0.064 ± 0.008	0.077 ± 0.010
NuWro (without FZ)	0.070	0.071
NuWro (with FZ)	0.079	0.077

TABLE XI. NC π^0 /CC ratio

peak of the pion momentum distribution to larger values by about 50 MeV/c resulting in much better agreement with the data.

Both MB and SciB experiments provide distributions of events versus the cosine of the angle between the neutrino and π^0 momenta. Figs 14 – 16 show pions angular distributions together with the NuWro predictions. We focus on the backward directions because we expect an important impact from FZ effects in this kinematical region.

Figs 14 and 15 show that the FZ increases the π^0 production in the backward directions but the effect is rather small. The reason is that at lower neutrino energies there are many backward moving π^0 's even without FSI effects.

We checked that only for larger Q^2 values the FSI become the main source of π^0 's and using the FZ reduces their number.

In the case of SciB experiment the NuWro results are normalized to the number π^0 predicted to be in the data. In this case using the FZ makes the absolute number of backward moving π^0 's little larger, but the effect can hardly be seen.

VI. CONCLUSIONS

Any comparison to recent NC π^0 production data requires a computational tool capable of modeling several dynamical mechanisms for neutrino-nucleon interaction as well as the FSI effects. The NuWro MC event generator has all the required physical models implemented and we have demonstrated that it reproduces the experimental results quite well. An important ingredient of the NuWro FSI model is the FZ mechanism which even at relatively small neutrino energies typical for K2K, MB and SciB experiments leads to observable effects on the π^0 's in the final state. We hope that our results will be useful for better evaluation of the systematic error coming from NC π^0 production in neutrino oscillation experiments like T2K.

ACKNOWLEDGMENTS

The authors were partially supported by the grants: N N202 368439 and 2011/01/M/ST2/02578.

-
- [1] H. Gallagher, AIP Conf. Proc. **1189** (2009) 35.
[2] A.M. Ankowski, PoS(NUFACT08) 118.
[3] P. de Perio, AIP Conf. Proc. **1405** (2011) 223.
[4] A. Ferrari, P.R. Sala, A. Fasso', and J. Ranft, CERN-2005-010, INFN/TC-05/11 (2005); G. Battistoni, P.R. Sala, M. Lantz, and G. Smirnov, Acta Phys. Pol. **B40** (2009) 2491.
[5] D. Casper, Nucl. Phys. B (Proc. Suppl.) **112** (2002) 161; P. Przewlocki, Acta Phys. Pol. **B40** (2009) 2513.
[6] Y. Hayato, Nucl. Phys. B (Proc. Suppl.) **112** (2002) 171; Acta Phys. Pol. B **40** (2009) 2477.
[7] C. Andreopoulos et al., Nucl. Instrum. Meth. **A614** (2010) 87.
[8] N. Metropolis et al., Phys. Rev. **110** (1958) 185 and 204;
[9] R.J. Glauber, in Lectures in Theoretical Physics, Vol. I, edited by W. E. Brittin and L. G. Dunham (Interscience, New York, 1959), p. 315.
[10] L. L. Salcedo, E. Oset, M. J. Vicente-Vacas, and C. Garcia-Recio, Nucl. Phys. **A484** (1988) 557
[11] A. H. Mueller, in Proceedings of the Seventeenth Rencontre de Moriond Conference on Elementary Particle Physics, Les Arcs, France, 1982 edited by J. Tran Thanh Van (Editions Frontieres, Gif-sur-Yvette, France, 1982); S. J. Brodsky, in Proceedings of the Thirteenth International Symposium on Multiparticle Dynamics, Volendam, The Netherlands, 1982, edited by W. Kittel et al. (World Scientific, Singapore, 1983).
[12] X.Qian, et al, Phys.Rev. **C81** (2010) 055209.
[13] L. Stodolsky, *Formation Zone Description in Multiproduction*, Talk at the VIIth International Colloquium on Multiparticle Reactions, Oxford, July 1975
[14] J. Ranft, Z. Phys. **C43** (1989) 439.
[15] V.V. Lyubushkin [NOMAD collaboration] Eur.Phys.J. **C63** (2009) 355.
[16] J.D. Zumbro et al, Phys. Rev. Lett **71** (1993) 1796; Bao-An Li, W. Bauer, and Che Ming Koa, Phys. Lett. **B382** (1996) 337; S.G. Mashnik, R.J. Peterson, A.J. Sierk, and M.J. Braunstein, Phys. Rev. **C61** (2000) 034601.
[17] C. Juszczak, J.A. Nowak, and J.T. Sobczyk, Nucl. Phys. B (Proc. Suppl.) **159** (2006) 211; J.A. Nowak, Phys. Scr. **T127** (2006) 70; C. Juszczak, Acta Phys. Pol. **B40** (2009) 2507;
[18] O. Benhar, A. Fabrocini, S. Fantoni, and I. Sick, Nucl. Phys. A **579** (1994) 493; D. Rohe et al. (E97-006 Collaboration), Phys. Rev. Lett. **93** (2004) 182501; D. Rohe, for the E97-006 Collaboration, Nucl. Phys. B (Proc. Suppl.) **159** (2006) 152.
[19] C. Juszczak, J. Nowak, and J.T. Sobczyk, Eur. J. Phys. **C39** (2005) 195.
[20] <http://gwdac.phys.gwu.edu/>
[21] C.H. Llewellyn Smith, Phys. Rep. **3** (1972) 261.

- [22] H. Budd, A. Bodek, and J. Arrington, *Modeling Quasi-elastic Form Factors for Electron and Neutrino Scattering*, hep-ex/0308005.
- [23] R. Bradford, A. Bodek, H.S. Budd, and J. Arrington, Nucl. Phys. Proc. Suppl. **159** (2006) 127.
- [24] W.M. Alberico, S.M. Bilenky, C. Giunti, and K.M. Graczyk, Phys. Rev. **C79** (2009) 065204.
- [25] A.M. Ankowski and J.T. Sobczyk, Phys. Rev. **C77** (2008) 044311.
- [26] T. de Forest, Jr., Nucl. Phys. **A392** (1983) 232.
- [27] H. F. Jones and M. D. Scadron, Ann. Phys. (N.Y.) **81** (1973) 1.
- [28] K.M. Graczyk, D. Kielczewska, P. Przewlocki, and J.T. Sobczyk, Phys. Rev. **D80** (2009) 093001.
- [29] D. Rein and L.M. Sehgal, Annals of Physics **133** (1981) 79.
- [30] K.M. Graczyk, C. Juszczak, and J.T. Sobczyk, Nucl. Phys. **A781** (2007) 227.
- [31] A. Bodek, U.K. Yang, Nucl. Phys. B Proc.(Suppl) **112** (2002) 70.
- [32] F. Sartogo, *Interazioni di neutrini atmosferici: un modello fenomenologico e la sua applicazione nell'interpretazione dei dati ottenibili in rivelatori sotterranei* (in Italian), PhD Thesis, supervisor P. Lipari, Rome; J.A. Nowak Phys. Scr. **T127** (2006) 70; J. Sobczyk, PoS(NUFACT08)141 (2008).
- [33] D. Rein and L.M. Sehgal, Nucl. Phys. **B223** (1983) 29.
- [34] E. Oset, L.L. Salcedo, D. Strottman, Phys. Lett. **B165** (1985) 13; E. Oset, L.L. Salcedo, Nucl. Phys. **A468** (1987) 631.
- [35] D. Ashery et al, Phys. Rev. **C23** (1981) 2173; D. Ashery et al, Phys. Rev. **C30** (1984) 946.
- [36] I. Navon, et al, Phys. Rev. **C28** (1983) 2548.
- [37] M.K. Jones et al, Phys. Rev. **C48** (1993) 2800.
- [38] R. A. Giannelli, et al, Phys. Rev. **C61** (2000) 054615.
- [39] S. M. Levenson, et al, Phys. Rev. **C28** (1983) 326.
- [40] L. Landau and I. Pomeranchuk, Doklady Akademii Nauk SSR **92** (1953) 535; *ibid* **92** (1953) 735.
- [41] A. Fasso et al, *The physics models of FLUKA: status and recent developments*, arXiv hep-ph/0306267.
- [42] P. Astier et al., [NOMAD Collaboration], Nucl. Phys. **B609** (2001) 255.
- [43] A. Bialas, Z. Phys. **C26** (1984) 301.
- [44] G. Battistoni, P.R. Sala, and A. Ferrari, Acta Phys. Pol. **B37** (2006) 2361.
- [45] G. Battistoni, A. Ferrari, A. Rubbia, and P.R. Sala, *The FLUKA nuclear cascade model applied to neutrino interactions*, talk given at NuInt02, <http://www.ps.uci.edu/~nuint/proceedings/sala.pdf>
- [46] D. S. Baranov, et al, *An Estimate For The Formation Length Of Hadrons In Neutrino Interactions*, PHE 84-04, 1984.
- [47] A. El-Naghy and S.M. Eliseev, J. Phys. G: Nucl. Part. Phys. **16** (1990) 39.
- [48] G. R. Farrar, H. Liu, L. L. Frankfurt, and M. I. Strikman, Phys. Rev. Lett. **61** (1988) 686.
- [49] W. Cosyn, M. C. Martinez, J. Ryckebusch, and B. Van Overmeire, Phys. Rev. **C74** (2006) 062201.
- [50] O. Buss et al, *Transport-theoretical Description of Nuclear Reactions*, to appear in Physics Reports, arXiv:1106.1344 [hep-ph].
- [51] Y. Hayato-san, private communication.
- [52] C. Andreopoulos et al, Nucl. Instrum. Meth. **A614** (2010) 87;
- [53] C. Andreopoulos, private communication.
- [54] G. Zeller, private communication.
- [55] P. Astier et al [NOMAD collaboration], Nucl. Phys. **B611** (2001) 3.
- [56] W. Krenz et al, Nucl. Phys. **B135** (1978) 45.
- [57] E.A. Hawker, *Single Pion Production in Low Energy ν Carbon Interactions*, talk given at NuInt02, <http://www.ps.uci.edu/~nuint/proceedings/hawker.pdf>. See also W. Lerche et al., Phys. Lett. **B78** (1978) 510.
- [58] S.L. Adler, S. Nussinov, and E.A. Paschos, Phys. Rev. **D9** (1974) 2125.
- [59] S. Nakayama et al. [K2K collaboration], Phys. Lett. **B619** 255.
- [60] A.A. Aguilar-Arevalo et al [MiniBooNE collaboration], Phys. Rev. **D81** (2010) 013005.
- [61] Y. Kurimoto, et al [SciBooNE collaboration], Phys. Rev. **D81** (2009) 033004.